

Reprocessing of X-rays in the outer accretion disc of the black hole binary XTE J1817–330

Marek Gierliński^{1*}, Chris Done¹ and Kim Page²

¹Department of Physics, University of Durham, South Road, Durham DH1 3LE, UK

Submitted to MNRAS

ABSTRACT

We build a simple model of the optical/UV emission from irradiation of the outer disc by the inner disc and coronal emission in black hole binaries. We apply this to the broadband *Swift* data from the outburst of the black hole binary XTE J1817–330 to confirm previous results that the optical/UV emission in the soft state is consistent with a reprocessing a constant fraction of the bolometric X-ray luminosity. However, this is very surprising as the disc temperature drops by more than a factor 3 in the soft state, which should produce a marked change in the reprocessing efficiency. The easiest way to match the observed constant reprocessed fraction is for the disc skin to be highly ionized (as suggested 30 years ago by van Paradijs), so that the bulk of the disc flux is reflected and only the hardest X-rays heat the disc. The constant reprocessed fraction also favours direct illumination of the disc over a scattering origin as the optical depth/solid angle of any scattering material (wind/corona) over the disc should decrease as the source luminosity declines. By contrast, the reprocessed fraction increases very significantly (by a factor ~ 6) as the source enters the hard state. This dramatic change is not evident from X-ray/UV flux correlations as it is masked by bandpass effects. However, it does not necessarily signal a change in emission e.g. the emergence of the jet dominating the optical/UV flux as the reflection albedo must change with the dramatic change in spectral shape.

Key words: X-rays: binaries – accretion, accretion discs

1 INTRODUCTION

Accreting black hole binaries radiate most of their energy in the X-ray bandpass, and the wealth of recent X-ray data means that their spectral behaviour in this energy range is well characterized. At high accretion rates (typically more than a few per cent of the Eddington luminosity) the accretion flow is dominated by an optically thick and geometrically thin disc, extending to the last stable orbit around the black hole. This disc emits most of its power at ~ 1 keV (Shakura & Sunyaev 1973), though it is always accompanied by a soft tail of emission to higher energies. By contrast, at lower luminosities the spectrum is dominated by a hard tail, usually attributed to Comptonization of soft seed photons in hot, optically thin plasma, peaking at ~ 100 keV. This soft-hard spectral transition indicates a change in the nature and geometry of the accretion flow, most plausibly due to the inner disc being evaporated into a radiatively inefficient flow (see e.g. the reviews by McClintock & Remillard 2006; Done, Gierliński & Kubota 2007). Strong evidence for this picture comes from the recent *Swift* monitoring campaign on the outburst of the low mass X-ray binary XTE J1817–330

(Rykoff et al. 2007, hereafter R07), where the low energy bandpass of the CCD detector gives for the first time a direct detection of the disc during the soft to hard transition and in the hard state (R07, Gierliński, Done & Page 2008, hereafter GDP08). While the derived inner disc radius is strongly model dependent in the hard state (simple fits indicate that the disc is not truncated while more complex models require a truncated disc: R07 and GDP08), all models give a larger inner radius in the transition spectra than in the soft state (R07, GDP08), as expected if a receding inner disc triggers the soft-hard transition (GDP08).

Studies of the corresponding radio behaviour tie the jet firmly into the accretion flow. The hard state has a steady jet whose radio power increases with the X-ray luminosity of the flow. This emission is suppressed in the soft, disc dominated state, but there can be strong radio flaring during rapid transitions from the hard to soft states. This is probably due to faster ejected material (perhaps the remains of the jet supporting, large scale height plasma from the low/hard state) catching up with the slower, steady jet from lower luminosity states, giving rise to strong shock acceleration (Fender, Belloni & Gallo 2004; Done et al. 2007).

By contrast with this wealth of data in the X-ray and radio bandpass, the optical is surprisingly poorly studied. There is

* E-mail:Marek.Gierlinski@durham.ac.uk

a broad consensus that the reprocessing of the soft X-ray emission from the outer disc should dominate the optical emission in the soft state (e.g. van Paradijs & McClintock 1994; Vrtilek et al. 1990; Esin et al. 2000; Hynes et al. 2002; 2005), but low/hard state is much less clear. There can still be an important contribution to the optical emission from reprocessed X-ray illumination of the outer disc (e.g. Esin et al. 2000) but the emission from the jet can also be important, as can the companion star (e.g. Russell et al. 2006). Disentangling these in an individual spectrum is not easy, but these models predict a different optical to X-ray luminosity ratio, L_O/L_X , from a series of spectra at different mass accretion rates. Theoretical models of the optical emission from irradiation and from the jet predict $L_O \propto L_X^{0.5}$ (van Paradijs & McClintock 1994) and $L_O \propto L_X^{0.7}$ (Russell et al. 2006), respectively. However, observations of a sample of low mass X-ray binaries (where the companion star should make negligible contribution to the optical emission except in quiescence) in the hard state shows $L_O \propto L_X^{0.6}$ law, roughly consistent with either disc reprocessing or the jet (Russell et al. 2006). Studies of the correlated X-ray/optical rapid (sub-second) variability seem to give a much better distinction between jet and disc models, since the disc reprocessing model gives a clear prediction that the optical light curve is a lagged and smeared version of the X-ray light curve. The lack of smearing of the lagged optical variability in the few cases where this has been attempted gives clear evidence for a jet contribution (Malzac et al. 2004; Gandhi et al. 2008).

Here we revisit the problem of disentangling the origin of the UV/optical emission from snapshot spectra. We again use the *Swift* data from the outburst of XTE J1817–330 (R07; GDP08) but this time focus on the simultaneous optical/UV photometry which accompanies each X-ray CCD spectrum. R07 showed that the UV flux tracks the square root of the 2–10 keV X-ray flux in all the data, and interpreted this as evidence for a reprocessing origin in both the soft and hard states. We build a simple physical model of reprocessing in the outer disc, and confirm the conclusion of R07 that this produces the optical/UV flux. However, we also show that simple flux–flux correlations mask a clear increase in fraction of bolometric flux which is required to be reprocessed and thermalized into the optical/UV as the source enters the hard state. While this could signal a switch to the jet dominating the optical/UV flux, we also show that this is also consistent with the same constant illuminating geometry as inferred for the soft state as the reflection albedo will change markedly for the changing spectral shape. However, it does also seem likely that there is a small jet contribution as well, since this is required by weak cross-correlation signal between the rapid optical and X-ray variability in a similarly bright hard state of GX339-4 (Gandhi et al. 2008).

We caution that the flux correlations resulting from reprocessing are not simple. More sophisticated physical models of X-ray illuminated discs are required in order to clearly predict the expected optical/UV flux from an irradiated disc, including the self-consistent vertical structure of the illuminated disc atmosphere, its reflection albedo and full emission spectrum (e.g. Jimenez-Garate et al. 2002). Only with such models will snapshot spectra be able to constrain the relative contribution of jet and illuminated disc in the hard state, and be able reliably estimate the solid angle of the directly illuminated outer disc.

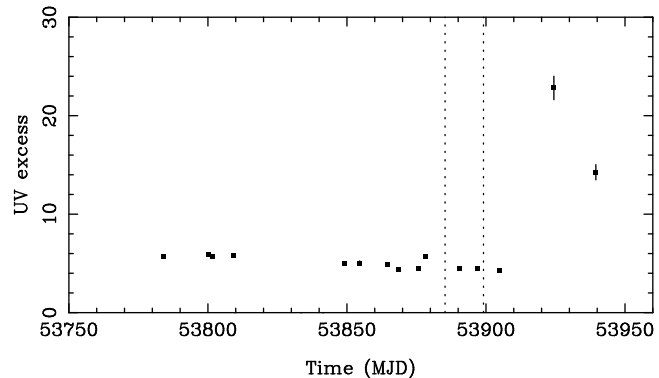


Figure 1. UV excess: the ratio of the UVOT flux in UVW1 filter divided by extrapolated DISKBB flux from best-fitting simple disc models to XRT data. Dotted lines separate X-ray spectral states: high/soft to the left, transition in the middle and low/hard to the right (see GDP08).

2 DATA REDUCTION

We use publicly available *Swift* data of the 2006 outburst of XTE J1817–330. We use the same X-ray telescope (XRT) spectra as in GDP08 (numbering follows that of R07, observation logs are presented in their tables 1 and 2 for details). Additionally, we extracted the corresponding UVOT data. The UVOT images were aspect-corrected and UVOT2PHA run to create XSPEC-compatible spectral points for every observation and filter. In each case, a 5-arcsec circle was used to extract the source counts, with a larger area used to estimate the contribution from the background.

We first give an overview of the optical/UV data by extrapolating the *Swift* XRT model fits to a standard disc (DISKBB) and Comptonization (THCOMP) (detailed in section 3.2 and table 1 of GDP08) down to the UVOT bandpass. We use the XSPEC model REDDEN to account for UV absorption, with fixed $E_{B-V} = 0.215$ mag (see R07). The X-ray fits always underpredict the optical/UV flux, and we quantify this by the ratio of the observed to extrapolated flux in the UVW1 filter of the UVOT. This ratio is plotted as a function of MJD in Fig. 1, showing that it remains relatively constant throughout the outburst in the high/soft and transition states (as defined in GDP08) but increases markedly in the low/hard state. The excess is highly significant irrespective of uncertainties in reddening e.g. in observation 1 the UV excess drops from 5.7 to 1.5 when E_{B-V} is changed from 0.215 to 0 mag. In the next section we build a physical model of the irradiated disc that can fit this observed UV excess.

3 IRRADIATED DISC MODEL

GDP08 showed how irradiation of the inner disc by the Compton tail could significantly change the temperature structure of the inner disc in the low/hard state. Neglecting this effect leads to an underestimate of the true inner disc radius compared to models which assume that gravitational energy release alone is responsible for the disc emission (R07). Here we concentrate on how this total emission (irradiated inner disc and Compton tail) can change the temperature structure of the outer disc by irradiation to produce the observed optical/UV emission.

We assume that the disc extends from R_{in} to R_{out} , and model the emission from gravitational energy release through viscosity

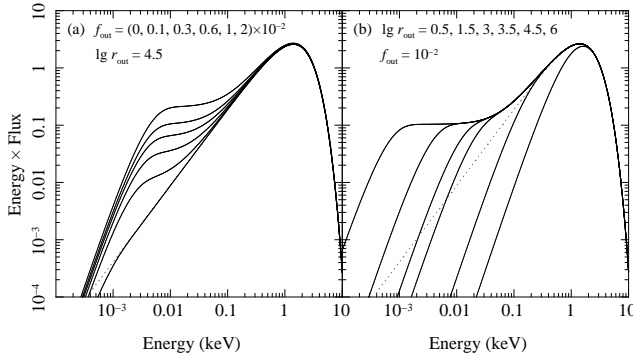


Figure 2. Model of the irradiated disc with no Comptonized tail (i.e. $L_c = 0$), as a function of irradiation fraction, f_{out} (left panel) and outer radius, r_{out} (right panel). The models (black solid lines) are calculated for $kT_{\text{in}} = 0.6$ keV. The left panel shows the effect of changing the fraction of the bolometric disc emission which is intercepted by the outer disc, from 0 (the lowest solid black line) to 0.02, for an assumed outer disc radius of $10^{4.5} R_{\text{in}}$. The right panel shows the effect of changing the outer disc radius from (right to left) $10^{0.5}$ to $10^6 R_{\text{in}}$ for a fixed illumination fraction of 0.01. The dotted grey line in both panels show a 0.6 keV DISKBB model (equivalent to $R_{\text{out}} = \infty$) for comparison.

using the simple DISKBB approach (stressed inner boundary condition) so that

$$Q_{\text{visc}} = \sigma T_{\text{disc}}^4 (R) = \frac{G M \dot{M}}{8\pi R^3} = \frac{L_d}{4\pi R_{\text{in}}^2} r^{-3} = \sigma T_{\text{in}}^4 r^{-3},$$

where $r \equiv R/R_{\text{in}}$ and

$$L_d = \frac{G M \dot{M}}{2R_{\text{in}}}$$

is the Newtonian expectation for the thin disc emission from gravitational energy release and

$$T_{\text{in}}^4 = \frac{L_d}{4\pi\sigma R_{\text{in}}^2}$$

is the temperature at the inner disc radius as parameterized in DISKBB model.

GDP08 considered the effect of irradiation of the disc by the Compton tail, with luminosity L_c . This irradiation will be most concentrated in the overlap region between the disc and hot flow, so given the uncertainties in geometry, GDP08 simply assumed that the irradiating flux was constant between R_{in} and R_{irr} and zero elsewhere. Then the reprocessed luminosity $L_{\text{rep}} = f_{\text{in}} L_c$, where f_{in} can be estimated via the albedo of the inner disc, a_{in} and the solid angle subtended by the overlap region to the X-ray source, $\Omega_{\text{in}}/2\pi$ as $f_{\text{in}} = (1 - a_{\text{in}})\Omega_{\text{in}}/4\pi \sim 0.1$, for typical hard state values of $a_{\text{in}} = 0.3$ and $\Omega_{\text{in}}/2\pi = 0.3$ (GDP08). This gives a flux at each irradiated part of the disc as

$$Q_{\text{rep}} = f_{\text{in}} \frac{L_c}{2\pi(R_{\text{irr}}^2 - R_{\text{in}}^2)} = 2\sigma T_{\text{in}}^4 f_{\text{in}} \frac{L_c}{L_d} \frac{1}{r_{\text{irr}}^2 - 1},$$

where $r_{\text{irr}} \equiv R_{\text{irr}}/R_{\text{in}}$.

Thus the total luminosity from the inner regions of the accretion disc is

$$L_{\text{bol}} = L_d + L_{\text{rep}} + L_c = L_d \left[1 + \frac{L_c}{L_d} (1 + f_{\text{in}}) \right].$$

This can in turn irradiate the outer disc, either directly if the disc shape is convex or warped, or by scattering if there is material

above the disc (such as the wind which is produced self consistently by X-ray irradiation e.g. Begelman, McKee & Shields 1983). We assume the illuminating flux is $f_{\text{il}} L_{\text{bol}} / (4\pi R^2)$, where f_{il} is a geometry-dependent illumination fraction (see also Dubus et al. 1999; Esin et al. 2000; Hynes et al. 2002). The R^{-2} gives a slower decline with radius than the R^{-3} dependence of the flux from intrinsic gravitational energy release. Thus at large radii irradiation must dominate over the intrinsic gravitational energy release (e.g. van Paradijs & McClintock 1994). Of this illuminating flux, a fraction a_{out} is reflected (a_{out} is the albedo of the outer disc), and a fraction η_{th} of the remaining absorbed flux is thermalized. We define the reprocessed fraction

$$f_{\text{out}} = f_{\text{il}} (1 - a_{\text{out}}) \eta_{\text{th}} \quad (1)$$

as the fraction of the bolometric flux which is thermalized in the disc. Finally, the total flux in the disc can be described by the following formula:

$$\begin{aligned} Q_{\text{tot}} = & \sigma T_{\text{in}}^4 \left\{ r^{-3} + f_{\text{out}} r^{-2} \left[1 + \frac{L_c}{L_d} (1 + f_{\text{in}}) \right] \right. \\ & \left. + \delta 2 f_{\text{in}} \frac{L_c}{L_d} \frac{1}{r_{\text{irr}}^2 - 1} \right\}. \end{aligned}$$

Here $\delta = 1$ for $r \leq r_{\text{irr}}$ and 0 otherwise.

This full model¹ has 8 free parameters. There are 4 defining the shape of the intrinsic spectrum (intrinsic disc temperature, Comptonization slope and electron temperature, and ratio of power in the disc and Comptonization components), and 2 defining the inner disc reprocessing (irradiation radius and fraction of flux intercepted). These are all constrained directly by the X-ray data, while the remaining 2 defining the outer disc reprocessing (outer radius of the disc and fraction of flux intercepted) are determined from the observed optical/UV emission.

We first set $L_c/L_d = 0$ to investigate the behaviour of pure disc self illumination. Fig. 2 shows the effect of changing f_{out} . The lowest solid curve shows the pure disc spectrum, while the dotted curve shows a comparison with DISKBB at the same temperature and inner disc radius. These are identical except at the lowest energies, as the bandpass is so wide that the outer disc radius (fixed at $\log r_{\text{out}} = 4.5$ in this plot) becomes important. Irradiation creates a characteristic ‘shoulder’ with flux $\propto f_{\text{out}} L_{\text{bol}} \nu^{-1}$ in the optical/UV. This shoulder extends between energies $3kT(r_{\text{trans}})$ and $3kT(r_{\text{out}})$, where r_{trans} is the radius at which there is the transition between irradiation and gravitational energy release. Below the shoulder, the flux is simply determined by the Rayleigh-Jeans tail of the irradiated outer disc so has flux $\propto \nu^2 T(r_{\text{out}}) \propto (f_{\text{out}} L_{\text{bol}} / r_{\text{out}}^2)^{1/4}$. Fig. 2b shows the effect of changing r_{out} . Irradiation has no effect on the disc emission if the disc is smaller than the radius at which irradiation dominates, whereas for a large disc the ‘shoulder’ can extend down into the IR.

We then extend the model to show the effect of including the Comptonization component on the outer disc illumination, including also its effect on the inner disc with $r_{\text{irr}} = 1.1$ and $f_{\text{in}} = 0.1$. The total bolometric luminosity (before reprocessing) is then $L_d + L_c$, and we assume that both disc and coronal flux are reprocessed in the same way, i.e. that a fraction f_{out} of the bolometric luminosity is thermalized in the outer disc. Fig. 3 shows a sequence of DISKIR models for various values of L_c/L_d . When $L_c/L_d = 0$ (thick blue solid line), the UV shoulder is produced by

¹ this model, `diskir`, is publicly available on the XSPEC web page <http://heasarc.gsfc.nasa.gov/docs/xanadu/xspec/newmodels.html>

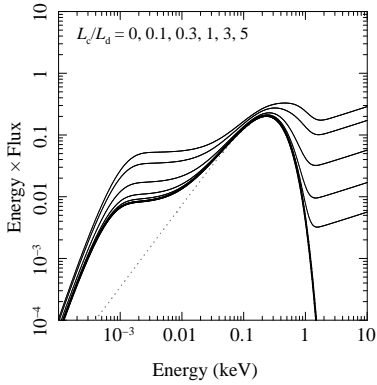


Figure 3. Model of the irradiated disc as a function of Comptonization-to-disk ratio, L_c/L_d . The model was calculated for $kT_{\text{in}} = 0.1$ keV, $f_{\text{out}} = 10^{-2}$, $r_{\text{ir}} = 1.1$, $\lg r_{\text{out}} = 4.5$, $\Omega/2\pi = 0.3$, $\Gamma = 1.7$ and $kT_e = 100$ keV. Solid lines show the models as a function of increasing parameter, from bottom to top (thicker curve corresponding to $L_c/L_d = 0$). The dotted grey line shows DISKBB model, i.e. the disc with no irradiation and extending to infinity. Note, that in a typical soft state ($L_c/L_d \ll 1$), the UV shoulder very weakly depends on the strength of the Comptonized tail, L_c/L_d , but it strongly depends on f_{out} (see Fig. 2).

the inner disc, L_d , irradiating the outer disc as in Fig. 2. The height of this shoulder does not strongly depend on L_c/L_d in the soft state, as this has $L_c/L_d < 1$ (by definition of soft state spectra). Hence the total bolometric luminosity is dominated by the constant L_d , so the reprocessed flux is likewise constant for a given f_{out} and r_{out} . However, for $L_c/L_d > 1$ then the bolometric luminosity increases substantially above L_d , so the reprocessed optical/UV emission likewise increases with the increase in illuminating flux.

4 RESULTS

We now use the irradiated disc model described in Section 3 to fit the data. We follow GDP08 and fix the shape of the Compton tail using the spectral index derived from the RXTE data and fix its electron temperature to 50 keV (thus the DTHIR model has only 6 free parameters). We start with observation 1, as it has the best signal-to-noise and also a full set of filters for the optical/UV coverage (V, B, U, UVW1, UVM2 and UVW2 i.e. spanning $\sim 2\text{--}8$ eV). Absorption by gas and dust in the interstellar medium affects the X-ray and UV/optical bandpass, respectively (described by the XSPEC model WABS and REDDEN). These two should be linked by a common dust-to-gas ratio, so we first explore the effect of this on the models.

Gorenstein (1975) found the relation between optical extinction, A_V , and Hydrogen column, $N_H = (2.2 \pm 0.3) \times 10^{21} A_V \text{ cm}^{-2} \text{ mag}^{-1}$ (see also Zombeck 1990). Taking the usual relation between extinction and colour excess (reddening), $A_V = 3.0 E_{B-V}$, this gives

$$E_{B-V}/N_H = (1.5 \pm 0.2) \times 10^{-22} \text{ cm}^2 \text{ mag}.$$

Other values quoted in literature are usually consistent with the above, e.g. Spitzer (1978) suggests $E_{B-V}/N_H = 1.7 \times 10^{-22} \text{ cm}^2 \text{ mag}$. We fit the first observation with three fixed values of $E_{B-V}/N_H = 1.3, 1.5$ and $1.7 \times 10^{-22} \text{ cm}^2 \text{ mag}$. In the fourth fit we allow for E_{B-V} to be a free parameter (independent of N_H). The results are shown in Table 1.

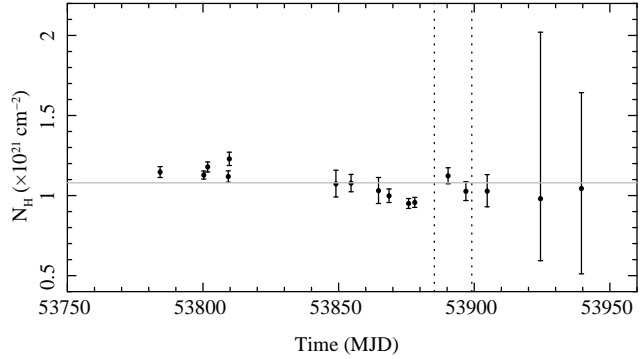


Figure 5. The best-fitting absorbing Hydrogen column from the irradiated disc model. The gray horizontal line shows the mean value of $N_H = 1.08 \times 10^{21} \text{ cm}^{-2}$. Vertical dotted lines separate the X-ray spectral states: HS is on the left, IM in the middle and LH on the right.

The model curves in Fig. 2 show that the main parameter controlling the amount of optical/UV flux is f_{out} , while r_{out} controls the optical/UV slope. Reddening has a fixed shape, so the amount of reddening mainly affects the total amount of flux, so should have most impact on f_{out} . This is supported by the results in Table 1, which show that the particular choice of colour excess has a large effect on the derived outer disc irradiation fraction, f_{out} , and a much smaller effect on r_{out} . It has no effect on any of the inner disc parameters or on N_H since these are set by the X-ray spectrum.

The clear tradeoff between the irradiation fraction and colour excess means that the absolute value of f_{out} cannot be constrained to better than within a factor ~ 2 . However, relative values can be constrained rather well assuming that there is no change in the absorption during the outburst. Hence we fix $E_{B-V}/N_H = 1.5 \times 10^{-22} \text{ cm}^2 \text{ mag}$ so that we can inspect trends in f_{out} throughout the outburst. We stress that in a typical soft state the UV shoulder is very weakly affected by the strength of the Comptonized tail (Fig. 3), so the measured values of f_{out} do not depend on a particular value of L_c/L_d , as long as it remains small (i.e. $\lesssim 0.2$).

We repeated this analysis for observations 2 and 3 as these are the only other observations with more than 2 filters present. Thus these are the only other spectra which can give constraints on the slope of the optical/UV spectrum and hence on r_{out} . These are both consistent with the $\log r_{\text{out}} = 4.5$ as found from observation 1, so we fix the outer disc radius at this value in all the datasets.

The outer disc radius of $r_{\text{out}} \equiv R_{\text{out}}/R_{\text{in}} \approx 10^{4.5}$ translates to a size scale of $3 \times 10^{11} \text{ cm}$ assuming a black hole mass of $M = 10 M_\odot$ and an inner disc radius of $6GM/c^2$. The disc size is set by tidal forces, which truncate the disc at roughly half the binary separation. Thus we can estimate that the orbital period should be about 20 hours, around the median period for the black hole binary systems (e.g. Remillard & McClintock 2006), and requiring a somewhat evolved companion star in order to fill its Roche lobe.

Now we fit the irradiated disc model to all the data sets, with all free model parameters detailed in Table 2. Fig. 4 shows the best-fitting model, data and residuals of representative spectra. Fig. 5 shows that the column density N_H is very well constrained by all the soft- and intermediate-state data, and is approximately consistent with a constant value of $N_H = (1.08 \pm 0.05) \times 10^{21} \text{ cm}^{-2}$. However, the hard state observations have much poorer signal to noise, so we fix the column at this value in the last two data sets in order to better constrain the remaining parameters.

N_H ($\times 10^{21} \text{ cm}^{-2}$)	E_{B-V}/N_H ($\times 10^{-22} \text{ cm}^2 \text{ mag}$)	kT_{in} (keV)	f_{out} ($\times 10^{-3}$)	$\lg r_{\text{out}}$	N_d ($\times 10^3$)	L_c/L_d	$\chi^2_{\nu}/\text{d.o.f.}$
1.16 \pm 0.04	(1.3)	0.890 \pm 0.016	0.69 \pm 0.05	4.50 \pm 0.05	2.62 \pm 0.16	0.11 \pm 0.03	601.3/542
1.16 \pm 0.04	(1.5)	0.890 \pm 0.016	0.89 \pm 0.07	4.46 \pm 0.05	2.62 \pm 0.16	0.11 \pm 0.03	605.4/542
1.16 \pm 0.04	(1.7)	0.890 \pm 0.016	1.2 \pm 0.1	4.44 \pm 0.04	2.62 \pm 0.16	0.11 \pm 0.03	610.3/542
1.16 \pm 0.04	0.9 \pm 0.3	0.890 \pm 0.016	0.36 $^{+0.20}_{-0.11}$	4.6 \pm 0.1	2.65 \pm 0.16	0.11 \pm 0.03	596.1/541

Table 1. Fit results of the irradiated disc model to observation 1 (UVOT and XRT spectra) showing the effect of reddening. The first three fits had E_{B-V} linked to N_H , while in the last fit E_{B-V} was free. The best-fitting value of the colour excess in the last fit was $E_{B-V} = (0.10 \pm 0.03)$ mag. N_H is the Hydrogen absorbing column, E_{B-V} reddening, T_{in} the intrinsic disc temperature at the inner radius, f_{out} the irradiation fraction, r_{out} the outer disc radius in units of inner radius, N_d is the disc component normalization (the same as in DISKBB) and L_c/L_d is the ratio of luminosity in the Comptonized component to that in the non-irradiated disc (i.e. intrinsic disc emission).

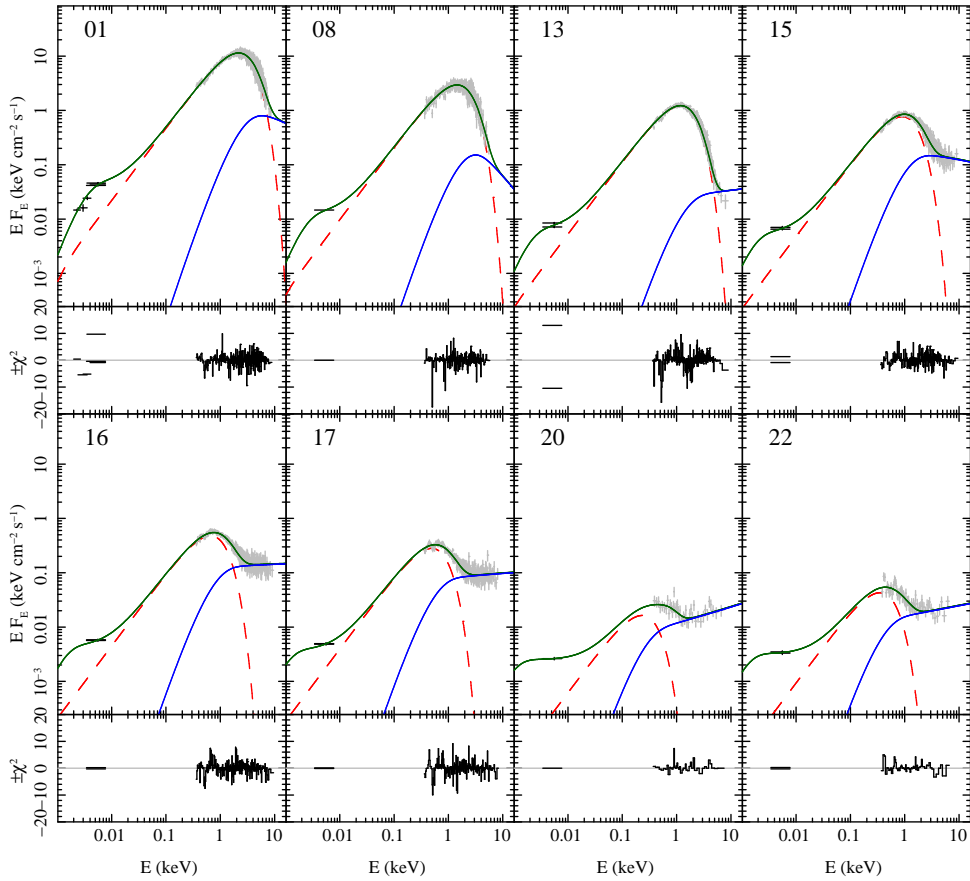


Figure 4. Representative spectra from UVOT and XRT with the best fitting models of the irradiated disc. Upper panels show the unfolded and unabsorbed spectra and models. Lower panels show the residuals, $\pm\chi^2 \equiv \text{sign}(\text{data}-\text{model})\chi^2$. In spectral panels UVOT data are shown in black, XRT data are in gray. The dashed red curve shows the intrinsic disc emission due to accretion (i.e. disc with no irradiation). The blue curve shows Comptonization, while the dark green curve the total spectrum, including Comptonization and irradiated disc. Observations 1, 8 and 13 were in the soft state, observations 15, 16 and 17 show the transition into the hard state, which is represented by the last two data sets 20 and 22.

The irradiation fraction, f_{out} , is shown as a function of time (Fig. 6), disc flux (Fig. 7), and Comptonization-to-disc ratio (Fig. 8). It remains remarkably constant at $f_{\text{out}} \sim 10^{-3}$, during the soft state and transition, but then jumps by a factor ~ 6 in the last two hard state spectra. Similar differences between the optical-X-ray correlation between hard and soft states are seen by Esin et al. (2000) and Maitra & Bailyn (2008). We stress again that while the absolute value of f_{out} is uncertain to within a factor 2, depending on the assumed reddening, the relative values are robust. It is also not dependent on the assumed Compton spectral shape at high

energies. Even for the hardest spectra, with $\Gamma = 1.75$, the bolometric luminosity only increases by a factor 1.3 by changing the high energy extent from ~ 150 keV (as produced by a 50 keV electron temperature) to 500 keV (more or less the maximum seen in X-ray binaries). This is much smaller than the factor 6 increase in flux required in order to make the irradiated fraction be consistent with that seen in the soft state. It is clear from Fig. 4 that the ratio of the observed UV/optical emission to that inferred for the underlying intrinsic (unirradiated) disc jumps markedly for the last two (hard state) spectra, though it is also clear that the first hard state spec-

Obs	N_H ($\times 10^{21}$ cm $^{-2}$)	kT_{in} (keV)	f_{out} ($\times 10^{-3}$)	N_d ($\times 10^3$)	Γ	L_c/L_d	$\chi_{\nu}^2/\text{d.o.f.}$
1	1.15 ± 0.03	0.894 ± 0.015	$0.86^{+0.05}_{-0.04}$	$2.6^{+0.2}_{-0.1}$	(2.34)	0.10 ± 0.03	607.1/543
2	$1.13^{+0.02}_{-0.03}$	$0.808^{+0.009}_{-0.008}$	0.99 ± 0.03	2.3 ± 0.1	(2.28)	0.05 ± 0.01	677.5/531
3	1.18 ± 0.03	0.78 ± 0.01	1.06 ± 0.04	2.6 ± 0.1	(2.34)	0.05 ± 0.02	558.4/499
4	$1.12^{+0.04}_{-0.03}$	0.70 ± 0.01	1.01 ± 0.04	3.0 ± 0.2	(2.31)	0.17 ± 0.02	520.0/488
5	1.23 ± 0.04	0.69 ± 0.01	1.08 ± 0.06	3.3 ± 0.2	(2.33)	0.19 ± 0.02	476.6/452
8	$1.07^{+0.09}_{-0.08}$	$0.60^{+0.03}_{-0.02}$	$1.00^{+0.08}_{-0.07}$	$3.3^{+0.6}_{-0.5}$	(3.00)	0.05 ± 0.04	352.5/289
9	1.08 ± 0.05	0.61 ± 0.01	0.99 ± 0.06	2.9 ± 0.2	(3.00)	0.01 ± 0.01	332.0/340
10	1.03 ± 0.08	$0.53^{+0.02}_{-0.01}$	$1.08^{+0.09}_{-0.08}$	3.2 ± 0.4	(1.99)	0.06 ± 0.03	297.8/260
11	1.00 ± 0.04	0.524 ± 0.008	$0.95^{+0.06}_{-0.05}$	$3.7^{+0.3}_{-0.2}$	(2.74)	0.04 ± 0.01	363.3/336
12	0.95 ± 0.03	0.512 ± 0.005	0.98 ± 0.05	$3.3^{+0.2}_{-0.1}$	(2.23)	0.04 ± 0.01	422.6/361
13	0.96 ± 0.03	0.498 ± 0.005	$1.21^{+0.06}_{-0.05}$	2.9 ± 0.1	(1.88)	0.06 ± 0.01	530.1/360
15	1.12 ± 0.05	0.381 ± 0.007	1.24 ± 0.08	5.5 ± 0.5	(2.15)	0.36 ± 0.02	412.6/367
16	1.03 ± 0.06	0.281 ± 0.006	$1.27^{+0.08}_{-0.07}$	$11.5^{+1.5}_{-1.3}$	(1.95)	0.73 ± 0.03	408.3/396
17	1.0 ± 0.1	0.208 ± 0.007	1.7 ± 0.1	23^{+5}_{-4}	(1.92)	0.89 ± 0.06	366.1/307
20	(1.08)	0.10 ± 0.02	$6.5^{+1.0}_{-0.9}$	26^{+26}_{-13}	(1.72)	$4.4^{+2.8}_{-1.2}$	39.9/40
22	(1.08)	0.15 ± 0.02	6.7 ± 0.8	13^{+8}_{-5}	(1.82)	$1.6^{+0.3}_{-0.2}$	66.1/65

Table 2. Fit results of the irradiated disc model, REDDEN*WABS*(DISKIR), using all available UVOT/XRT data. Parameters are as in Table 1, with fixed $E_{B-V}/N_H = 1.5 \times 10^{-22}$ cm 2 mag and $\lg r_{\text{out}} = 4.5$. Γ is the photon spectral index of the Comptonized component, derived from the PCA data (see GDP08).

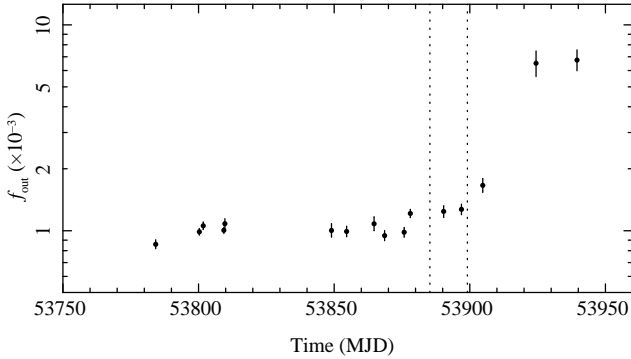


Figure 6. Irradiation fraction, f_{out} , during the outburst. Dotted lines separate the X-ray spectral states: HS is on the left, IM in the middle and LH on the right.

trum (observation 17) is consistent with the soft and intermediate states.

As discussed in Section 3, the UV shoulder does not depend on L_c/L_d in the soft state. However, during the transition and in the hard state, where $L_c/L_d \gtrsim 1$, the UV shoulder is shaped both by f_{out} and L_c/L_d (see Fig. 3). Nonetheless, the X-ray spectral shape constrains L_c/L_d , and with this then even a single UV data point independently constrains f_{out} . This is the case even for the hard state, as shown by the lack of correlation between these parameters in observation 22 (Fig. 9), showing that the hard-state increase in f_{out} is real (Fig. 8).

5 UV/X-RAY CORRELATION

The previous section showed that there is a robust change in the ratio of UV/optical to X-ray flux in the hard state compared to that seen in the soft and transition states, indicating a change in either the geometry or radiative process (see also Esin et al. 2000). This is initially surprising, as R07 showed that the 2–10 keV X-ray lumi-

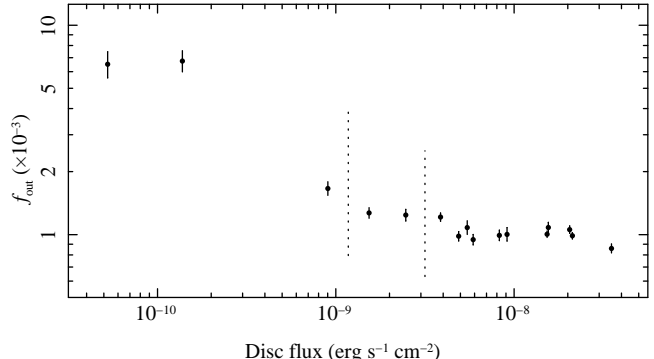


Figure 7. Irradiation fraction, f_{out} , as a function of disc flux. Dotted lines separate the X-ray spectral states: HS is on the right, IM in the middle and LH on the left.

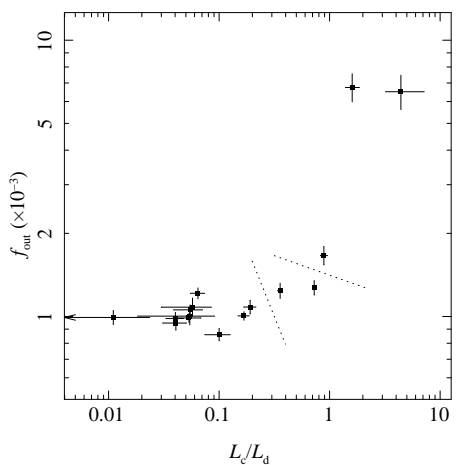


Figure 8. Irradiation fraction, f_{out} , as a function of the Comptonization-to-disc ratio, L_c/L_d from irradiated disc fitted to UVOT/XRT data.

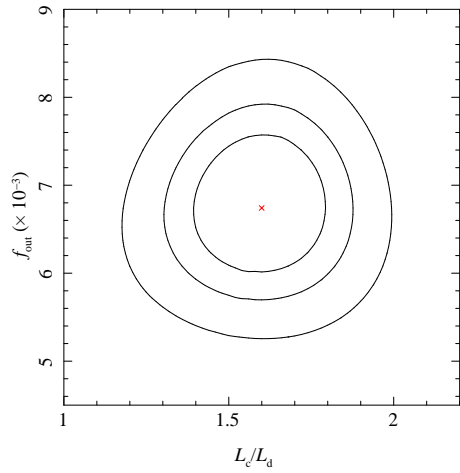


Figure 9. Contour plot of χ^2 as a function of f_{out} and L_c/L_d for observation 22, using irradiated disc model (see Fig. 8). The cross shows the χ^2 minimum and the contours correspond to (innermost first) 68, 90 and 99 per cent confidence level.

nosity, L_{2-10} , was related to the UV luminosity in the UVW1 filter as $L_{\text{UVW1}} \propto L_{2-10}^{0.5}$ throughout the outburst, with the hard states following the same correlation as the soft. This is the relationship predicted from reprocessing by van Paradijs & McClintock (1994), but only in the special case where the filter samples the turnover between the ‘shoulder’ ($\text{flux} \propto L_{\text{bol}}$) and the Rayleigh-Jeans tail from the outer edge of the disc ($\propto L_{\text{bol}}^{0.25}$, see Section 3). Yet the derived disc size in these data is fairly large, and the UVW1 filter used for the correlation is mostly on the irradiation dominated shoulder rather sampling the outer disc Rayleigh-Jeans tail (see Fig. 4). Thus the models predict that reprocessing should give $L_{\text{UVW1}} \propto L_{\text{bol}}$ rather than $\propto L_{\text{bol}}^{0.5}$.

However, the 2–10 keV flux is not a good tracer of the bolometric flux. Even in the soft state, the changing disc temperature means that the 2–10 keV spectrum is initially dominated by the high temperature disc while the Compton tail becomes more important as the disc temperature decreases (see Fig. 4). Thus there is a variable bolometric correction for the 2–10 keV flux even in the soft state spectra.

We show all these effects explicitly by simulating the spectrum of an irradiated disc for typical soft state spectral parameters (inner and outer radii fixed at $N_d = 3000$ and $r_{\text{out}} = 10^{4.5}$, weak Compton tail of $L_c/L_d = 0.05$ and $\Gamma = 2.2$) with fixed $f_{\text{out}} = 10^{-3}$ (see Table 2). The thick curve in Fig. 10 (marked as S_{2-10}) shows the effect of changing the disc temperature in this model from 0.9 keV to 0.3 keV. This is approximately described by $L_{\text{UVW1}} \propto L_{2-10}^{0.5}$, while the 0.3–10 keV flux, which more closely follows the bolometric flux, gives $L_{\text{UVW1}} \propto L_{2-10}^{0.8}$ (actually closer to the ‘jet signature’). The approximate ‘reprocessing signature’ of van Paradijs & McClintock (1994) is coincidentally recovered in the data by masking the true reprocessing flux relation by the changing spectral shape in the X-ray bandpass!

The changing shape of the X-ray spectrum is of course accentuated during the state transition. Fig. 10 shows the effect of keeping the irradiated fraction constant ($f_{\text{out}} = 10^{-3}$) while changing the spectral shape to a typical hard state spectrum ($kT_{\text{in}} = 0.1$ keV, $N_d = 20000$, $\Gamma = 1.75$ and $L_c/L_d = 5$). If we used the full bolometric flux for the correlation, this point should lie on the same line as the soft-state correlation. However, when the X-ray flux is

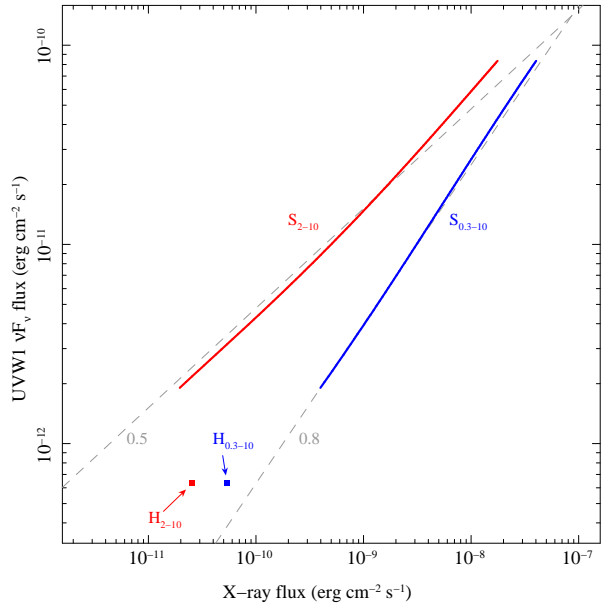


Figure 10. X-ray/UV flux correlation simulated using the irradiated disc model. The UV flux corresponds to the UVW1 filter of *Swift*/UVOT detector, i.e. integrated flux from 3.4 to 7.7 eV. The X-ray flux is either 2–10 or 0.3–10 keV flux. Gray dashed lines in the background show power laws with indices 0.5 and 0.8. The thick curves (marked as S_{2-10} in red and $S_{0.3-10}$ in blue) represent the soft state correlation. They were modelled for typical soft-state parameters (see Table 2) of $L_c/L_d = 0.05$, $\Gamma = 2.2$, $N_d = 3000$, $f_{\text{out}} = 10^{-3}$ and kT_{in} varying from 0.3 to 0.9 keV. The two points (pointed by arrows and marked as H_{2-10} and $H_{0.3-10}$) show how the hard state would look like if it had the same irradiation fraction as the soft state, $f_{\text{out}} = 10^{-3}$. The other parameters for the hard state model were $L_c/L_d = 5$, $N_d = 20000$ and $kT_{\text{in}} = 0.1$ keV.

used (in particular 2–10 keV flux) the hard state point does not lie on extrapolation of the soft state (the point marked as H_{2-10} in Fig. 10). This change in spectral shape between hard and soft states then predicts that there is a change in the optical-X-ray flux correlation measured over a fixed bandpass. Such an effect is clearly seen by Maitra & Bailyn (2008) in the neutron star transient Aql X-1.

The observed hard state, unlike this simulation, follows the soft-state correlation (R07). This is possible only when there is an increase in irradiated flux to counteract the large decrease in bolometric correction. This manifests itself in the increase of measured irradiation fraction in the hard state (see Fig. 8).

We strongly caution against using optical/UV–X-ray flux–flux correlations as a diagnostic of the origin of the optical flux. The ‘reprocessing signature’ of $L_{\text{opt}} \propto L_{2-10}^{0.5}$ is only very approximate, depending on the size of the disc and the changing bolometric correction from L_{2-10} depending on spectral shape (especially if there are spectral transitions).

6 DISCUSSION

Swift observations of XTE J1817–330 during its outburst clearly show that the UV emission is in excess of a simple extrapolation of the standard multicolour blackbody disc fitting the X-ray band (R07). This is as expected from irradiation of the outer disc by the intense X-ray emission produced in the inner disc. We develop a self-consistent model of the X-ray spectrum, where the broadband optical/UV/X-ray spectrum is made up from four components, the

intrinsic dissipation in the disc, the Compton tail, irradiation of the inner disc by the tail, and irradiation of the outer disc by all of the above.

The outer disc can be irradiated in two different ways. Firstly, a wind or corona can form above the disc and scatter the central X-rays down. As discussed in section 3, the fraction f_{out} of the central luminosity that is reprocessed, thermalized and reemitted as blackbody (defined by equation 1) depends on the fraction which illuminates the disc, f_{il} , the fraction of this which is absorbed, $(1 - a_{\text{out}})$, and the fraction of this absorbed flux which thermalizes, η_{th} . In case of the scattering wind/corona the geometry-dependent factor is

$$f_{\text{il}} = \frac{\Omega_{\text{sc}}}{2\pi} \tau_{\text{sc}},$$

where Ω_{sc} is the solid angle of the wind/corona seen by the central source and τ_{sc} is the optical depth of the wind/corona along the line of sight from the central source. In case of direct irradiation the illumination fraction is simply

$$f_{\text{il}} = \frac{\Omega_{\text{out}}}{2\pi},$$

where Ω_{out} is the solid angle of the outer disc seen by the central source.

The most intriguing result reported in this paper is constancy of f_{out} in the soft state. The disc temperature changes by a factor 3, the Comptonization-to-disc ratio varies by an order of magnitude, the bolometric luminosity changes dramatically, while the reprocessed fraction remains fairly constant at $f_{\text{out}} \sim 10^{-3}$. This is possible only when the albedo, a_{out} , the thermalization fraction, η_{th} , and the illumination fraction, f_{il} , remain constant throughout the soft state. The alternative is a fine tuning of the above parameters to maintain a constant f_{out} .

Here we discuss constancy of these three quantities and draw possible physical scenarios for the irradiation of the outer disc in XTE J1817–330 in the soft spectral state.

6.1 Illumination geometry: soft state

X-ray illumination heats the top skin of the disc up to the Compton temperature, and this material escapes as a wind if the thermal velocity at this temperature is faster than the escape velocity (Begelman et al. 1983). Simulations show that the column density and solid angle of this wind give $f_{\text{il}} = (\Omega_{\text{sc}}/2\pi)\tau_{\text{sc}} \sim L/L_{\text{Edd}}$ (Woods et al. 1996). However, this wind is produced only at large radii, above $\sim 2 \times 10^{10} T_{\text{IC},8}^{-1}$ cm for a $10M_{\odot}$ black hole, where $T_{\text{IC},8}$ is the Compton temperature in units of 10^8 K (Begelman et al. 1983). The Compton temperature is about a half of the disc temperature for soft state spectra, so even at the outburst peak with the disc at 0.9 keV this gives $T_{\text{IC},8} \sim 0.05$. That makes the radius at which the wind can be produced comparable to our estimate of the outer disc radius of 3×10^{11} cm. Hence, it seems likely that the disc is too small to effectively drive a powerful wind.

Instead, an X-ray heated (static) corona develops above the disc. It can still scatter flux down onto the disc and this scattered fraction should still strongly depend on the irradiating flux i.e. be $\propto L/L_{\text{Edd}}$. Fully iterative calculations of the self consistent vertical structure produced by an X-ray illuminated disc are complex (e.g. Jimenez-Garate, Raymond & Liedahl 2002), but this material is observed in the highly inclined neutron star systems (the accretion disc corona and dipping sources). The compilation of dipping sources by Díaz Trigo et al. (2006) shows a persistent (non-dip)

column density of $\sim(4-10) \times 10^{22}$ cm $^{-2}$ of photoionized material along the line of sight for neutron stars with $L/L_{\text{Edd}} \sim 0.02-0.2$. The solid angle of this material is probably ~ 0.1 (e.g. Frank, King & Lasota 1987), hence the illumination fraction should be $(\Omega_{\text{sc}}/2\pi)\tau_{\text{sc}} \sim (3-7) \times 10^{-3}$. This number can be consistent with the observed f_{out} , depending on the actual value of a_{out} and η_{th} (see Section 6.2), but it should *decrease* by an order of magnitude as the luminosity declines. This contradicts the observations.

Hence it seems more likely that the disc is directly illuminated, where the constant illumination fraction, $\Omega_{\text{out}}/2\pi$, is a natural consequence of a constant disc geometry. Detailed calculations show that the (steady state) disc shape is convex, so a pure disc cannot self-illuminate (Dubus et al. 1999), but the self-consistent X-ray illuminated disc vertical structure is more complex, and can lead to a thicker disc (Jimenez-Garate et al. 2002; Loska, Czerny & Szczepański 2004). Alternatively, the disc can be warped, so that the outer edge is directly illuminated. Such warps are inferred from the long term periods seen in some X-ray binary light curves (e.g. Tananbaum et al. 1972) and may be produced simply by irradiating the disc (Peterson 1977; Pringle 1996).

6.2 Albedo and thermalization fraction: soft state

The reflection albedo and fraction of non-reflected flux which can thermalize are both strongly depend on the vertical structure of the disc. Material at the local blackbody temperature is effectively neutral in terms of soft X-ray opacity, so soft X-rays are absorbed rather than reflected. Thus the decreasing disc temperature as the soft state declines predicts a decreasing reflection albedo. We can estimate the albedo for any of our model spectra by convolving them with the neutral reflection code REFLECT in XSPEC. The range of soft-state spectra used in Fig. 10 (i.e. decreasing temperature from 0.9 to 0.3 keV with constant $L_{\text{c}}/L_{\text{d}} = 0.05$) give an albedo which decreases from ~ 0.02 to 0.008. These albedos are so small that the change in absorbed flux, which is $\propto (1 - a_{\text{out}})$, is negligible.

This does not necessarily imply that the reprocessed flux should be a constant fraction of the bolometric luminosity. The strongly increasing opacity at softer X-ray energies seen in neutral material also means that the softest X-rays are absorbed at such small depths in the disc that their luminosity does not thermalize. Instead of forming a blackbody spectrum, the energy is emitted predominantly as line and recombination continuum above the Lyman limit. Thus the reprocessed emission in the optical/UV is only a very small fraction of the total reprocessed flux. Conversely, hard X-rays penetrate deeper down into the disc, and thermalize (e.g. Suleimanov et al. 1999).

The thermalization fraction can be estimated as the fraction of luminosity emitted above 2 keV, $\eta_{\text{th}} \sim L_{2-\infty}/L_{\text{bol}}$. This factor changes from 0.4 to 0.05 as the soft state temperature changes from 0.9 to 0.3 keV (the highest and lowest temperature in the soft state models of Fig. 10). Thus the combined effect of albedo and thermalization in neutral material means that the reprocessed flux should change by a factor $\sim (1 - a_{\text{out}})\eta_{\text{th}} \approx \eta_{\text{th}}$, i.e. by a factor 8. Our observation of a constant f_{out} then requires that the illumination fraction, f_{il} , increases by this amount to offset the changing thermalization fraction! This seems very contrived.

Instead, it seems more likely that the X-ray illumination produces a thin ionized skin over the disc. This increases its albedo to close to unity in the limit where skin is completely ionized so that only the energy from the very hardest X-rays is not reflected due to Compton down-scattering. This conclusion is strengthened as sim-

ilarly high albedo is also inferred from the lack of irradiation of the companion star. This implies that the disc opening angle is at least 15° , so the outer disc solid angle is not negligibly small. The only way to the explain the observed weak optical emission from reprocessing is if most of the X-rays are reflected (van Paradijs 1983; van Paradijs & McClintock 1994).

Only the highest energy X-rays are absorbed by such a highly reflective disc, and these form only a small fraction of the illuminating flux in the soft state which may remain constant as the soft state declines. All this flux thermalizes so $\eta_{\text{th}} \sim 1$ and $f_{\text{out}} = f_{\text{il}}(1 - a_{\text{out}})\eta_{\text{th}} \sim f_{\text{il}}(1 - a_{\text{out}}) \ll 1$. Our value of $f_{\text{out}} = 10^{-3}$ implies that the disc intercepts a fraction $f_{\text{il}} \approx 2 \times 10^{-2}$ of the total bolometric flux for $a_{\text{out}} = 0.95$ (van Paradijs & McClintock 1994).

6.3 Hard State

The constant reprocessed fraction, f_{out} , seen in the soft state is most easily interpreted if the outer disc is directly illuminated and has a constant albedo and thermalization efficiency. The latter two conditions are probably easier to achieve if the disc has an ionized skin (self-consistently produced by the illumination: Jiminez-Garate et al. 2002). If so, the spectral change to the hard state will produce a large change in albedo as the luminosity of the hard state peaks at energies around 100 keV where Compton down-scattering means that the energy must be absorbed by the disc. The minimum albedo for the hard state spectra is around ~ 0.6 even for completely ionized material, thus we expect an apparent increase in reprocessed flux by a factor ~ 6 for a soft state albedo of ~ 0.95 , as observed! Thus it seems most likely that there is no change in reprocessing geometry as the source makes a transition to the hard state, but that there is a change in albedo.

7 CONCLUSIONS

We develop a simple physical model of an X-ray illuminated disc, where some fraction of the bolometric luminosity (both the disc and Comptonized tail) can illuminate the outer disc. We assume that such cool material has a reflection albedo which is around ~ 0.3 and that all the non-reflected luminosity can thermalize to the local blackbody temperature. Fitting this to the broadband optical/UV/X-ray *Swift* spectra of the outburst of the black hole binary XTE J1817–330 shows that the optical/UV emission in the soft state is consistent with a reprocessing of a constant fraction of the bolometric X-ray luminosity. This argues against a scattering origin for the illumination, as the optical depth/solid angle of a wind/corona from the disc should decrease as the source luminosity declines. Instead it is much more likely that the outer disc is directly illuminated by the central source, and maintains a constant opening angle throughout the soft state. However, we estimate that for neutral material the reflection albedo should be very small, and the thermalization fraction should change markedly as the soft state declines, requiring a fine tuned increase of the irradiation geometry in order to produce the constant reprocessed fraction. Instead it seems more likely that there is an ionized skin which develops over the disc, giving a much higher reflection albedo and a constant thermalization fraction. If so, then the change in albedo which results as the source makes the transition to a hard state spectrum can explain the apparent jump in fraction of reprocessed flux at this point with a constant reprocessing geometry. This would argue against a significant additional contribution from the jet to this hard state optical/UV emission.

These results highlight the additional physical insight which is derived from fitting even simple physical models of an illuminated disc as opposed to flux-flux correlations. We urge further development of more sophisticated models which properly include the albedo and thermalization effects now that such excellent data are available to constrain the illumination geometry of the outer disc.

ACKNOWLEDGEMENTS

MG and CD acknowledge support through a Polish MNiSW grant NN203065933 (2007–2010) and STFC Senior Fellowship, respectively.

REFERENCES

Begelman M. C., McKee C. F., Shields G. A., 1983, ApJ, 271, 70
 Díaz Trigo M., Parmar A. N., Boirin L., Méndez M., Kaastra J. S., 2006, A&A, 445, 179
 Done C., Gierliński M., Kubota A., 2007, A&ARv, 15, 1 (DGK07)
 Dubus G., Lasota J.-P., Hameury J.-M., Charles P., 1999, MNRAS, 303, 139
 Esin A. A., Kuulkers E., McClintock J. E., Narayan R., 2000, ApJ, 532, 1069
 Fender R. P., Belloni T. M., Gallo E., 2004, MNRAS, 355, 1105
 Frank J., King A. R., Lasota J.-P., 1987, A&A, 178, 137
 Gandhi P., et al., 2008, MNRAS, L87
 Gierliński M., Done C., Page K., 2008, MNRAS, 388, 753 (GDP08)
 Gorenstein P., 1975, ApJ, 198, 95
 Hynes R. I., 2005, ApJ, 623, 1026
 Hynes R. I., Haswell C. A., Chaty S., Shrader C. R., Cui W., 2002, MNRAS, 331, 169
 Jimenez-Garate M. A., Raymond J. C., Liedahl D. A., 2002, ApJ, 581, 1297
 Loska Z., Czerny B., Szczepański R., 2004, MNRAS, 355, 1080
 Maitra D., Bailyn C. D., 2008, ApJ, in press, (arXiv:0807.3542)
 Malzac J., Merloni A., Fabian A. C., 2004, MNRAS, 351, 253
 McClintock J. E., Remillard R. A., 2006, in: *Compact stellar X-ray sources*. W. Lewin, M. van der Klis (Eds.). Cambridge Astrophysics Series, No. 39, Cambridge University Press, 157
 Petterson J. A., 1977, ApJ, 216, 827
 Pringle J. E., 1996, MNRAS, 281, 357
 Remillard R. A., McClintock J. E., 2006, ARA&A, 44, 49
 Russell D. M., Fender R. P., Hynes R. I., Brocksopp C., Homan J., Jonker P. G., Buxton M. M., 2006, MNRAS, 371, 1334
 Rykoff E. S., Miller J. M., Steeghs D., Torres M. A. P., 2007, ApJ, 666, 1129 (R07)
 Shakura N. I., Syunyaev R. A., 1973, A&A, 24, 337
 Spitzer L., 1978, *Physical Processes in the Interstellar Medium*. Wiley, New York
 Suleimanov V., Meyer F., Meyer-Hofmeister E., 1999, A&A, 350, 63
 Tananbaum H., Gursky H., Kellogg E. M., Levinson R., Schreier E., Giacconi R., 1972, ApJ, 174, L143
 van Paradijs J., 1983, *Accretion-driven stellar X-ray sources*, Cambridge University Press, Cambridge, 189
 van Paradijs J., McClintock J. E., 1994, A&A, 290, 133
 Vrtilek S. D., Raymond J. C., Garcia M. R., Verbunt F., Hasinger G., Kurster M., 1990, A&A, 235, 162
 Woods D. T., Klein R. I., Castor J. I., McKee C. F., Bell J. B., 1996, ApJ, 461, 767
 Zdziarski A. A., Gierliński M., 2004, PThPS, 155, 99
 Zdziarski A. A., Johnson W. N., Magdziarz P., 1996, MNRAS, 283, 193
 Zombeck M. V., 1990, *Handbook of space astronomy and astrophysics*. Cambridge Univ. Press, Cambridge